ELSEVIER

Prolate spheroidal wave functions, an introduction to the Slepian series and its properties

Ian C. Moore [a,*] and Michael Cada [b,c]

[a] *Queens University, Department of Mathematics and Statistics, Kingston, Ontario, Canada K7L 3N6*
[b] *University of Ottawa, School of Information Technology and Engineering (SITE), Ottawa, Ontario, Canada K1N 6N5*
[c] *Dalhousie University, Department of Computer and Electrical Engineering, Halifax, Nova Scotia, Canada B3J 1Z1*

Abstract

For decades mathematicians, physicists, and engineers have relied on various orthogonal expansions such as Fourier, Legendre, and Chebyschev to solve a variety of problems. In this paper we exploit the orthogonal properties of prolate spheroidal wave functions (PSWF) in the form of a new orthogonal expansion which we have named the Slepian series. We empirically show that the Slepian series is potentially optimal over more conventional orthogonal expansions for discontinuous functions such as the square wave among others. With regards to interpolation, we explore the connections the Slepian series has to the Shannon sampling theorem. By utilizing Euler's equation, a relationship between the even and odd ordered PSWFs is investigated. We also establish several other key advantages the Slepian series has such as the presence of a free tunable bandwidth parameter.
© 2004 Elsevier Inc. All rights reserved.

Keywords: Interpolation; Orthogonal expansion; Prolate spheroidal wave function

1. Introduction

Claude E. Shannon once posed the question: To what extent are functions, which are confined to a finite bandwidth also concentrated in the time domain? This raised the interests of three researchers at Bell Laboratories in the late fifties: D. Slepian, H.O. Pollack, and H.J. Landau. David Slepian discovered that the prolate spheroidal function of order zero, $S_{0n}(t)$, is maximally concentrated within a given time interval [9–11,18–20]. From this he discovered a new set of band limited functions rich in a unique

---

* Corresponding author.
  E-mail addresses: icmoore@mast.queensu.ca (I.C. Moore), mcada@site.uottawa.ca, michael.cada@dal.ca (M. Cada).

combination of properties, which are normalized versions of $S_{0n}(t)$, and recognized them as prolate spheroidal wave functions, conventionally abbreviated to PSWFs. Slepian was also the first to note the connection between PSWFs and the integral equation in the middle of the 20th century.

Trigonometric functions are orthogonal and complete over a finite interval; however, unlike trigonometric or any other set of functions, PSWFs have the liberty of forming an orthonormal basis set over infinity as well. Another property that gives them their appeal is that their Fourier transform over a finite and infinite interval is a scaled version of itself [4].

The properties inherent to these functions have intrigued researchers for decades in which many have attempted to find a method of exploiting them. Throughout the years, the inventors of PSWFs as well as many others have focused their attention on their time/bandlimited characteristics. We, however, shift our attention to the orthogonal properties of these functions. Within the last few decades, discrete prolate spheroidal sequences (DPSS) have been found to have applications in digital signal processing. This is where DPSSs of the zeroth order are found to be optimal windows in finite impulse (FIR) filter design [13,15,22]. DPSSs have also been found to be the optimal set of window tapers for Thomson's multitaper spectrum estimation method [16]. PSWFs are not to be confused with DPSSs. Both PSWFs and DPSSs are however very similar where by DPSSs are, connotatively speaking, a derivative of PSWFs with DPSSs being easier to compute and are only known over a finite interval [16]. The computation of PSWFs is not trivial and the complexity of their derivation has been the primary reason for their absence from the engineering and scientific arenas. With today's computational processing speeds this no longer poses a problem.

In the context of generalized analysis and synthesis, we can conventionally decompose functions into a linear combination of coefficients by the following means:

$$f(t) = \sum_{n=0}^{\infty} \gamma_n \phi_n(t), \tag{1}$$

where $f(t)$ is our function, γ_n is a set of scalar coefficients and $\phi_n(t)$ is an orthogonal basis set. As it is well known, the coefficients can be computed in the following fashion:

$$\gamma_n = \frac{\langle f(t)\phi_n(t) \rangle}{\langle \phi_n(t)\phi_n(t) \rangle}. \tag{2}$$

Some popular basis sets for performing this analysis is the Legendre, Chebyschev, and Fourier series. In this paper we highlight PSWFs as being a new alternative choice for analysis decomposition and synthesis. Since PSWFs were primarily the work of David Slepian [18–20], in this paper we name this orthogonal expansion the Slepian series.

Section 2 begins with some notation used in this paper and some unique properties of PSWFs. This is followed by Section 3 with a review of the historical foundations of the origins of PSWFs coupled with an explanation of various derivations of PSWFs. In Section 4 we expand on the orthogonal properties of PSWFs and utilize them in the form of the Slepian series. Several other analytical concepts are also outlined. In Section 5 we show the relationship between the odd and even orders of adjacent PSWFs by utilizing Euler's equation.

Within the last few years there have been some contributions to the understanding of interpolation with PSWFs in the publications of Walter [23] and Xiao [24,25]. Also, with regards to interpolation, we further develop the ideas of Walter in Section 6 with the use of this tool as we probe the importance of the bandwidth parameter of PSWF. We also empirically show a smaller error in the recovery of a given

function when tested against Fourier series interpolation. With regards to the approach of Xiao, we make conceptual comparisons to the generalized analysis/synthesis approach. By utilizing the Slepian series we show in Section 7 that a convergence to the Shannon sampling theorem is achieved under certain parameter settings.

In Section 8 we analytically determine the energy of the square wave approximation.

Finally, in Section 9 we empirically demonstrate the performance of the Slepian series. With regards to approximation of discontinuous functions such as the square wave or the Gaussian function we show that the Slepian series converges faster than other conventional orthogonal expansions such as the Fourier, Legendre, and Chebyschev.

2. Notation and properties

In the next few sections we follow the notation of Flammer [3] and Slepian [18,19] where PSWFs as a set of bandlimited functions are given the conventional notation of $\psi_n(t)$ on the continuous domain. Although the conventional notation shows a dependency on two parameters, PSWFs are actually dependent on a total of four parameters: the continuous time parameter t, the order, n, of the function, the interval on which the function is known, t_0, and the bandwidth parameter c. The bandwidth parameter is given by

$$c = t_0 \Omega, \tag{3}$$

where Ω is the finite bandwidth or cutoff frequency of $\psi_n(t)$ of a given order n.

In most of the literature, the parameter c is suppressed in the notation. In this paper it contributes much to the Slepian series so we add it in and name it the Slepian frequency. Since the theory was implemented in a discrete manner, we discard the conventional continuous notation and later in Sections 4–9 we use

$$\psi_n(c, kT) = \psi_{n,c}[k], \tag{4}$$

where T is the sampling period, c is a real positive value (Slepian frequency), n is the integer order and k is the integer time sample number. Also, the following notation is defined:

$$f(kT) = y[k], \tag{5}$$

where $y[k]$ is the discrete version of continuous $f(t)$.

The PSWFs $\psi_n(c, t)$ concentrated in the interval of $[-t_0, t_0]$ are normalized eigenfunctions of the system

$$\int_{-t_0}^{t_0} \psi_n(c, t) \frac{\sin \Omega(x - t)}{\pi(x - t)} \, dt = \psi_n(c, x) \lambda_n(c), \tag{6}$$

where $\lambda_n(c)$ is the eigenvalue of the sinc kernel and can be also regarded as the index of concentration on the interval $[-t_0, t_0]$. For the sake of simplicity we set the concentration interval to $[-1, 1]$ in our implementation, as did the authors of [23,24]. The eigenfunctions $\psi_n(c, t)$ are invariant to a finite Fourier transform

$$\int_{-t_0}^{t_0} \psi_n(c, t) e^{jwt} \, dt = j^n \left(\frac{2\pi \lambda_n(c) t_0}{\Omega} \right)^{1/2} \psi_n\left(c, \frac{wt_0}{\Omega} \right). \tag{7}$$

The infinite Fourier transform of $\psi_n(c, t)$ is also invariant

$$\int_{-\infty}^{\infty} \psi_n(c, t) e^{jwt} \, dt = j^n \left(\frac{2\pi t_0}{\Omega} \right)^{1/2} \psi_n \left(c, \frac{wt_0}{\Omega} \right). \tag{8}$$

This shows that $\psi_n(c, t)$ are doubly invariant to the Fourier transform. This invariance for both the finite and infinite domain states that $\psi_n(c, t)$ is bandlimited.

Another key set of properties states that $\psi_n(c, t)$ also obey a duality of orthogonality where the eigenfunctions of (6) are orthogonal over a finite and infinite domain. These functions are also normalized so that the following inner products obey the following:

$$\int_{-t_0}^{t_0} \psi_n(c, t) \psi_m(c, t) \, dt = \begin{cases} \lambda_n(c) & \text{for } n = m, \\ 0 & \text{otherwise,} \end{cases} \tag{9}$$

$$\int_{-\infty}^{\infty} \psi_n(c, t) \psi_m(c, t) \, dt = \begin{cases} 1 & \text{for } n = m, \\ 0 & \text{otherwise.} \end{cases} \tag{10}$$

With (10) we can represent any infinite continuous function $f(t)$ as in (1) where the coefficients are given by

$$\gamma_n(c) = \int_{-\infty}^{\infty} f(t) \psi_n(c, t) \, dt. \tag{11}$$

This naturally obeys the Parseval's equality,

$$\sum_{n=0}^{\infty} (\gamma_n(c))^2 = \int_{-\infty}^{\infty} |f(t)|^2 \, dt. \tag{12}$$

The convergence of the series is given by [18]

$$\lim_{N \to \infty} \int_{-\infty}^{\infty} \left[f(t) - \sum_{n=0}^{N} \gamma_n(c) \psi_n(c, t) \right]^2 \, dt = 0. \tag{13}$$

From this $f(t)$ can be closely approximated for all t and with N from (13)

$$f(t) \simeq \sum_{n=0}^{N} \gamma_n(c) \psi_n(c, t). \tag{14}$$

This kind of approximation is good for functions whose energy is distributed over the infinite time domain. For realistic applications we are more concerned with close approximations to a high degree of precision over a finite domain whose energy is not maximally concentrated about any given point. We address this in Section 4 where we find our way around this issue.

3. Derivation of prolate spheroidal wave functions

There are several ways to generate the function set, each having its advantages and disadvantages in complexity and precision [3,7,18,24]. Within the last ten years, computer processing speeds have climbed to the point where generating the function set is not an issue when it comes to their study. It becomes difficult when implementing an algorithm that generates the function set over its domain for higher orders of n and high bandwidth values of c. For this, the best approach is the following expansion:

$$\psi_n(c, t) = \sum_{k=0}^{\infty} \beta_k^n P_k(t). \tag{15}$$

$P_n(t)$ is the normalized Legendre polynomial of order n. The coefficients β_k^n can be calculated from the following recurrence relation:

$$\frac{(k+2)(k+1)}{(2k+3)\sqrt{(2k+5)(2k+1)}} c^2 \beta_{k+2}^n + \left(k(k+1) + \frac{2k(k+1)-1}{(2k+3)(2k-1)} c^2 - \chi_j \right) \beta_k^n$$
$$+ \frac{k(k-1)}{(2k-1)\sqrt{(2k-3)(2k+1)}} c^2 \beta_{k-2}^n = 0, \tag{16}$$

where χ_i are the eigenvalues, the derivation of which is discussed in [25].

For this paper we have adopted the same approach in the derivation as did Slepian and Flammer [3,14,18], which uses the angular and radial solutions in spheroidal wave coordinates of the first kind to the Helmoltz wave equation. The following procedure was cross-referenced and numerically verified by the tabulator results found in [1,3,5,18,21]. To find the eigenvalue in (9), we use the radial solution in spheroidal wave coordinates of the Helmoltz wave equation of the first kind

$$\lambda_n(c) = \frac{2c}{\pi} \left[R_{0n}(c, 1)^2 \right]. \tag{17}$$

A table of computationally derived eigenvalues can be found in Tables 5 and 6.

For the evaluation of $\psi_n(c, t)$, we used the angular solution of the Helmoltz wave equation of the first kind

$$\psi_n(c, t) = \frac{\sqrt{\lambda_n(c)/t_0}}{\mu_n(c)} S_{0n}\left(c, \frac{t}{t_0} \right), \tag{18}$$

where

$$\mu_n(c) = \sqrt{\int_{-1}^{1} \left(S_{0n}(c, t) \right)^2 dt}.$$

From (18) we can see the origins of Slepian's reasoning as to his claim that $\psi_n(c, t)$ are simply normalized versions of the spheroidal wave functions of order zero. To find the solution $S_{0n}(c, t)$, we apply the following expansion:

$$S_{mn}(c, t) = \sum_{r=0,1}^{\infty} d_r^{mn}(c) P_{m+r}^m(t). \tag{19}$$

$P_{m+r}^m(t)$ is the Legendre polynomial while $d_r^{mn}(c)$ represents the expansion coefficient. There are several approaches to attaining this coefficient (see [3,21]); they are classically determined in the following manner:

$$X_k d_{k+2}^{mn}(c) + (Y_k - A_{mn}) d_k^{mn}(c) + Z_k d_{k-2}^{mn}(c) = 0, \tag{20}$$

where

$$X_k = \frac{(2m + k + 2)(2m + k + 1)}{(2m + 2k + 3)(2m + 2k + 5)} c^2, \tag{21}$$

$$Y_k = (m + k)(m + k + 1) + \frac{2(m + k)(m + k + 1) - 2m^2 - 1}{(2m + 2k - 1)(2m + 2k + 3)} c^2, \tag{22}$$

$$Z_k = \frac{k(k - 1)}{(2m + 2k - 3)(2m + 2k - 1)} c^2. \tag{23}$$

For the scheme above we solved the recurrence in an iterative fashion.

The expansion for the radial solution $R_{mn}(c, \varepsilon)$ of the first kind was determined in the following manner:

$$R_{mn}(c, \varepsilon) = \frac{u_{m,n}(c, \varepsilon)}{\sum_{r=0,1}^{\infty} d_r^{mn}(c)((2m + 1)!)/r!} \left(\frac{\varepsilon^2 - 1}{\varepsilon^2} \right)^{1/2m}, \tag{24}$$

where

$$u_{m,n}(c, \varepsilon) = \sum_{r=0,1}^{\infty} i^{r+m-n} d_r^{mn}(c) \frac{(2m + r)!}{r!} j_{m+r}(c, \varepsilon). \tag{25}$$

The term $j_{p(z)}$ is a scaled spherical Bessel function $B_p(v)$ of the first kind

$$j_{m+r}(c, \varepsilon) = \sqrt{\frac{\pi}{2c\varepsilon}} B_{m+r+1/2}(c, \varepsilon). \tag{25}$$

The characteristic value A_{mn} of (20) was found iteratively. The numerical procedure can be found in [26] along with the numerical procedure for the expansion coefficients of $d_r^{mn}(c)$. An efficient implementation of these expansion coefficients can also be found in [12].

This approach to generate $\psi_n(c, t)$ was used in the numerical experimentation to attain the results of Section 9. This procedure is only valid for time values within the bounds of $[-1, 1]$. For the determination of $\psi_n(c, t)$ outside the bounds of $[-1, 1]$, the following scheme can be applied:

$$\psi_n(c, t) = \left(\frac{\lambda_n(c)}{t_0 N_n} \right)^{1/2} \kappa_n \sum_{r=0,1}^{M(n)} (-1)^{(r-n)/2} d_r^{0n}(c) j_r \left(\frac{ct}{t_0} \right). \tag{26}$$

$j_r(z)$ are the spherical Bessel functions as above; for determination of the normalization constant N_n, the κ_n factor and the truncation number $M(n)$, see [4].

4. Slepian series

Looking back at (11) we see that if a function $f(t)$ is known over infinity, then it can be synthesized by a set of coefficients. Using (14), the function can be closely reconstructed. For practical applications we

are more concerned with data over finite domains. Using (9) and applying the principles of Eq. (2), we can synthesize any continuous bandlimited function $f(t)$ by a set of coefficients determined by a finite interval employing the following:

$$\gamma_n(c) = \lambda_n^{-1}(c) \int_{-t_0}^{t_0} f(t)\psi_n(c,t)\,dt. \tag{27}$$

The function can then be reconstructed using the expansion (1) yielding what we call a Slepian series synthesis

$$f(t) \simeq \sum_{n=0}^{N} \gamma_n(c)\psi_n(c,t). \tag{28}$$

Equations (27) and (28) can be regarded as a synthesis and analysis pair for finite length continuous functions. Originally the authors of [4,18] intended these equations to have applications in signal extrapolation. This is a problem which has been studied [2,17] but has yet to be fully thought out and implemented. This is mainly attributed to the lack of understanding of PSWFs outside the $[-t_0, t_0]$ interval. Due to the orthogonal nature of $\psi_n(c,t)$, these equations can be viewed upon in much the same way as other more popular orthogonal expansion routines.

In this paper we make numerical comparisons between the convergence of the Slepian series and three other more popular orthogonal expansions. These expansions are:
the Fourier series,

$$a_n = \frac{1}{L} \int_{-L}^{L} f(t)\cos\left(\frac{\pi n t}{L}\right)dt, \tag{29}$$

$$b_n = \frac{1}{L} \int_{-L}^{L} f(t)\sin\left(\frac{\pi n t}{L}\right)dt, \tag{30}$$

$$f(t) \simeq \sum_{n=0}^{N} a_n\cos\left(\frac{\pi n t}{L}\right) + b_n\sin\left(\frac{\pi n t}{L}\right), \tag{31}$$

the Legendre series,

$$a_n = \frac{2n+1}{2} \int_{-1}^{1} P_n(t)f(t)\,dt, \tag{32}$$

$$f(t) \simeq \sum_{n=0}^{N} a_n P_n(t), \tag{33}$$

and the Chebyschev series,

$$a_n = \frac{1}{M} \sum_{k=-M}^{M} f(t_k)T_n(t_k)\,dt, \tag{34}$$

$$f(t) \simeq \left[\sum_{n=0}^{N-1} a_n T_n(t) \right] - \frac{a_0}{2}. \tag{35}$$

$P_n(t)$ are Legendre polynomials and $T_n(t)$ are Chebyschev polynomials. The set $\{t_{-M}, \ldots, t_M\}$ in (34) represents the zero crossings of $T_N(t)$.

Loosely speaking orthogonal expansions work best on functions that resemble its orthogonal basis set. It is well known that the Fourier synthesis (31) is optimally suited for periodic functions while Chebyschev synthesis (35) works extremely well with polynomial functions. With the Slepian synthesis it is not known where it is optimally suited for. In Section 9 we empirically show that it converges very well with the Gaussian function and the discontinuous square wave function.

The optimal truncation value has been well studied for various orthogonal expansions such as Fourier, Chebyschev, and Legendre. To get some insight of the optimal truncation value for the Slepian series we go to the work of [11] to understand the behavior of the eigenvalues $\lambda_n(c)$.

As the order n increases, the energy of the functions $\psi_n(c, t)$ becomes less concentrated in the interval $[-1, 1]$ for fixed values of c. A good measure of this is the numerical value of the eigenvalue $\lambda_n(c)$. Since the functions $\psi_n(c, t)$ posses this kind of behavior for increasing order n, the summation of the eigenvalues is a finite value [25]

$$\sum_{n=0}^{\infty} \lambda_n(c) = \frac{2c}{\pi}. \tag{36}$$

The first $\lceil (2c)/\pi \rceil$ eigenvalues are close to 1 by a small difference δ, where $\delta > 0$; therefore

$$\lambda_n(c) < (1 - \delta) \quad \text{whenever } n \leqslant \left\lceil \frac{2c}{\pi} \right\rceil. \tag{37}$$

For n beyond $\lceil (2c)/\pi \rceil$ the eigenvalues quickly descend close to 0 yet never reaching it. For $\delta \simeq 0$, close to all the energy in $\psi_n(c, t)$ of a given order n for all $t \in [-1, 1]$ is contained within that boundary [11]. To get a good idea of this refer to Tables 5 and 6 for a listing of various energy indexes (i.e., $\lambda_n(c)$) for PSWFs of various orders of n and values of c.

By applying the analysis of finite length function in (27) and the sum of the eigenvalues of (36), using Parseval's equality of (12) we can state

$$\int_{-t_0}^{t_0} |f(t)|^2 \, dt > \sum_{n=0}^{\lceil (2c)/\pi \rceil} \lambda_n(c) |\gamma_n(c)|^2. \tag{38}$$

This says that the energy contained in the function $f(t)$ will obey the following truncation condition:

$$N > \left\lceil \frac{2c}{\pi} \right\rceil, \tag{39}$$

where N is the truncation value. From this one can see that c shares some relationship with the number of coefficients used in the set.

If we look at the Fourier series synthesis, we see that it is broken into two Eqs. (29) and (30). The orthogonal basis set of (29) uses cosine, which are even functions and the orthogonal basis set of (30) uses sine, which are odd functions. Naturally, (29) can be used to synthesize even functions and (30) can be used to synthesize odd functions. PSWFs also exhibit similar behaviors of symmetry. Referring

to Figs. 3 and 4 one can see that the even orders of $\psi_n(c, t)$ are even and the odd orders of $\psi_n(c, t)$ are odd. The rules of symmetry that apply to the Fourier series also apply in the same manner to the Slepian series. Using analysis and synthesis equations of (27) and (28), respectively, one obtains for the analysis

$$p_n(c) = \lambda_{2n}^{-1}(c) \int_{-t_0}^{t_0} f(t)\psi_{2n}(c, t)\, dt, \tag{40}$$

$$q_n(c) = \lambda_{2n+1}^{-1}(c) \int_{-t_0}^{t_0} f(t)\psi_{2n+1}(c, t)\, dt, \tag{41}$$

and for the synthesis

$$f(t) \simeq \sum_{n=0}^{N'} p_n(c)\psi_{2n}(c, t) + q_n(c)\psi_{2n+1}(c, t), \tag{42}$$

where

$$N' > \left\lceil \frac{c}{\pi} \right\rceil. \tag{43}$$

The analysis of (42) and (43) can be represented in a discrete sense as

$$p_n(c) = \frac{t_0}{M\lambda_{2n}(c)} \sum_{k=-M}^{M} y[k]\psi_{2n,c}[k], \tag{44}$$

$$q_n(c) = \frac{t_0}{M\lambda_{2n+1}(c)} \sum_{k=-M}^{M} y[k]\psi_{2n+1,c}[k], \tag{45}$$

and for the synthesis

$$y[k] \simeq \sum_{n=0}^{N'} p_n(c)\psi_{2n,c}[k] + q_n(c)\psi_{2n+1,c}[k]. \tag{46}$$

The value M is the number of samples and was chosen to obey the Nyquist sampling theorem; the sampling period T is then

$$T = \frac{t_0}{M}. \tag{47}$$

When deciding on how to go about using the Slepian analysis, there are two parameters to consider: the number of Slepian coefficients N' and the Slepian frequency c. With most orthogonal analysis, one needs only to decide on the number of analysis coefficients N. With the Slepian series, one of the unique characteristics that distinguishes it from the Fourier series is the presence of a free parameter, c. Due to its significance we have decided to name it the Slepian frequency. Choosing the optimal Slepian frequency value c is an issue and is not trivial. However, (39) can be used as a general guide to choosing the correct c and N.
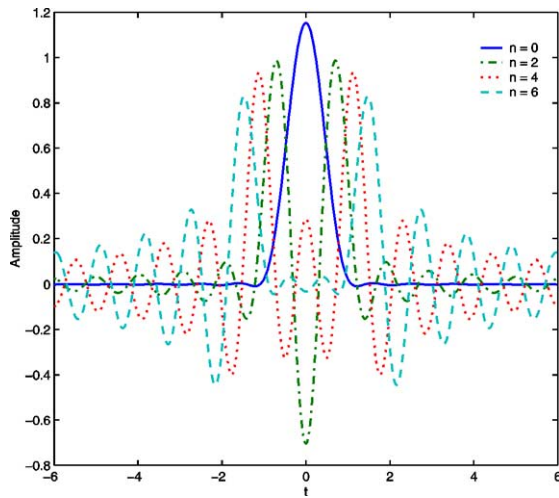
Fig. 1. $\psi_n(6, t)$ of even order n.
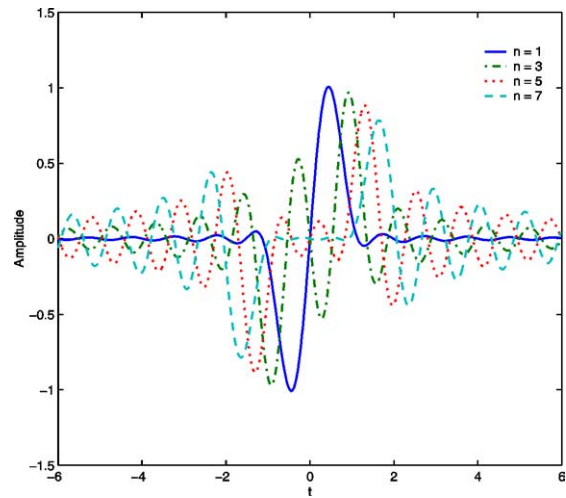
Fig. 2. $\psi_n(6, t)$ of odd order n.
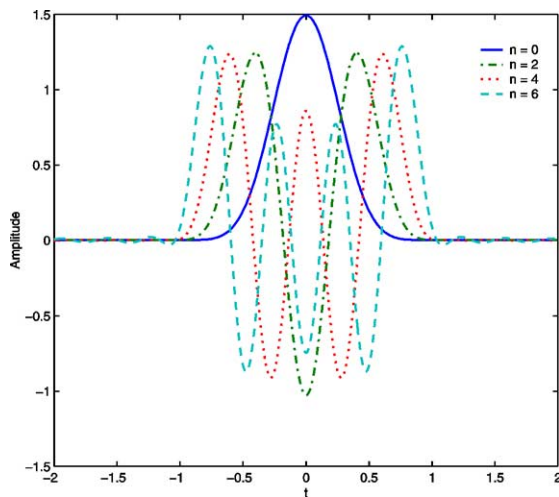
Fig. 3. $\psi_n(16, t)$ of even order n.
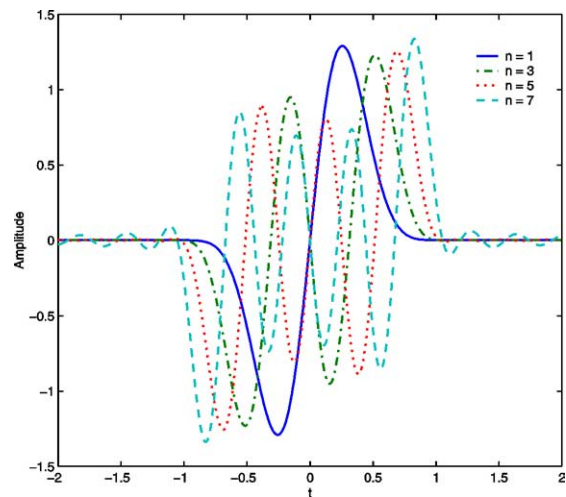
Fig. 4. $\psi_n(16, t)$ of odd order n.

5. Symmetry and aperiodic behavior

There has not been much attention drawn to the symmetry of $\psi_n(c, t)$ although David Slepian discusses some issues in [19]. As shown in the previous section, the Slepian analysis of (27) can be segmented into two distinct coefficient sets representing the even (40) and odd (41) components of a signal $f(t)$. In this section we attempt to draw a relationship between the even and odd functions of $\psi_n(c, t)$.

As an example, Figs. 3 and 4 show that the various orders of the functions $\psi_n(c, t)$ are aperiodic, and that the oscillation frequency increases with the value c. Conventionally, when we study cyclic behavior or any type of motion, trigonometric functions are used. Cyclic patterns are by nature—most of

the time—aperiodic, yet we as engineers, physicists, and mathematicians model these patterns with the periodic trigonometric functions. The Slepian series offers a new alternative. The relationship between cosine and sine has been very well studied. Due to their periodic nature, understanding the relationship between sine and cosine is trivial. If we look at the equation $\cos^2(t) + \sin^2(t) = 1$, it can be viewed from several perspectives: the parametric equation of the unit circle, the magnitude of the eigenfunction $e^{j\theta}$ or the trigonometric Pythagorean identity. If we apply these lines of thinking to the odd and even sets of $\psi_n(c, t)$ the outcome is not as trivial. Consider the following analogous expression:

$$\psi_{2n}^2(c, t) + \psi_{2n+1}^2(c, t) = K_n^2(c, t). \tag{48}$$

Using a counter example one can write

$$\psi_{2n}^2(c, t) + \psi_{2n+1}^2(c, t) = k,$$

where k is constant. Integrating the above equation with respect to t

$$\int_{-\infty}^{\infty} \psi_{2n}^2(c, t)\, dt + \int_{-\infty}^{\infty} \psi_{2n+1}^2(c, t)\, dt = \int_{-\infty}^{\infty} k\, dt,$$

one obtains using (10)

$$2 \neq \infty.$$

This equivalently leads to the energy of $K_n(c, t)$ being

$$\int_{-\infty}^{\infty} \left| K_n(t) \right|^2 dt = \int_{-\infty}^{\infty} \left| \sqrt{\psi_{2n}^2(c, t) + \psi_{2n+1}^2(c, t)} \right|^2 dt = \int_{-\infty}^{\infty} \psi_{2n}^2(c, t)\, dt + \int_{-\infty}^{\infty} \psi_{2n+1}^2(c, t)\, dt = 2.$$

If one plots the parametric relationship of sine and cosine one obtains the unit circle, while plotting the parametric relationship of (48) yields a convergent system shown in Fig. 5. If we regard the horizontal axis as real and the vertical axis as imaginary, the relationship between odd and even orders of $\psi_n(c, t)$ can be expressed in Euler's format

$$\psi_{2n}(c, t) + j\psi_{2n+1}(c, t) = \left| K_n(c, t) \right| e^{j\theta_n(c,t)}, \tag{49}$$

where the phase is defined by

$$\theta_n(c, t) = \tan^{-1} \frac{\psi_{2n+1}(c, t)}{\psi_{2n}(c, t)}, \tag{50}$$

while the magnitude is $|\sqrt{\psi_{2n}^2(c, t) + \psi_{2n+1}^2(c, t)}|$. To see a graphical relationship of $K_n(c, t)$ and $\theta_n(c, t)$ plotted against t refer to Figs. 6 and 7, respectively.

As t of the aperiodic system of 5 reach infinity, the points within the neighborhood of the origin stays nearby and approaches the origin. This system would fit the definition of an attractor [6]. The radial distance from the origin to any given point of corresponding t on the attractor plot is the value $|K_n(c, t)|$, which can be regarded as the magnitude of the symmetry pair. The angle between the radial arm and the horizontal axis can be regarded as the phase, $\theta_n(c, t)$, of the symmetry pair.
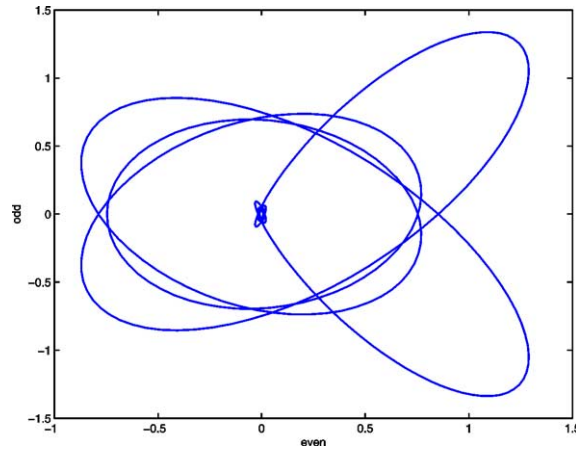
Fig. 5. Parametric plot, $(\psi_6(16,t))^2 + (\psi_7(16,t))^2 = (K_3(16,t))^2$.
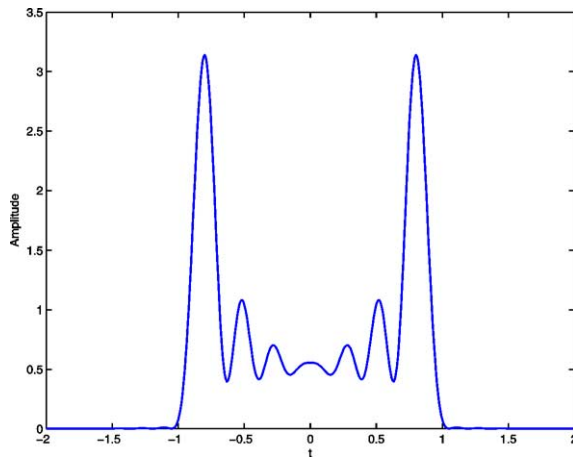
Fig. 6. Magnitude, $|K_3(16,t)|$.
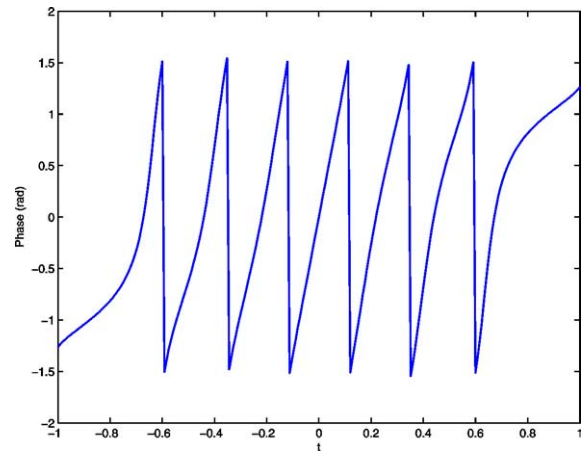
Fig. 7. Phase, $\theta_3(16,t)$.

Using (49) one would only need $N/2$ orders of $K_n(c,t)$ for the analysis instead of using N orders of $\psi_n(c,t)$. The Slepian analysis for signals of infinite length becomes

$$\gamma_n(c) = \int_{-\infty}^{\infty} f(t)K_n(c,t)e^{j\theta_n(c,t)}\,dt. \tag{51}$$

For signals of finite length, the eigenvalue $\lambda_n(c)$ must be considered

$$\left(\frac{\psi_{2n}(c,t)}{\lambda_{2n}(c)}\right)^2 + \left(\frac{\psi_{2n+1}(c,t)}{\lambda_{2n+1}(c)}\right)^2 = \left(K_n'(c,t)\right)^2. \tag{52}$$

Using the above, (49) becomes

$$\frac{\psi_{2n}(c,t)}{\lambda_{2n}(c)} + j\frac{\psi_{2n+1}(c,t)}{\lambda_{2n+1}(c)} = \left|K_n'(c,t)\right|e^{j\theta_n'(c,t)}. \tag{53}$$

Using $K_n'(c,t)$ the Slepian analysis for signals of finite length becomes

$$\gamma_n(c) = \int\limits_{-t_0}^{t_0} f(t) K_n'(c,t) e^{j\theta_n'(c,t)} \, \mathrm{d}t, \tag{54}$$

where the phase is defined by

$$\theta_n'(c,t) = \tan^{-1} \frac{\lambda_{2n}(c) \psi_{2n+1}(c,t)}{\lambda_{2n+1}(c) \psi_{2n}(c,t)}. \tag{55}$$

6. The Slepian series as an interpolator

The idea of using PSWFs to recover one-dimensional discrete functions has been previously explored by Xiao [24] and Walter [23]. Both authors approached the problem from slightly different perspectives where Walter's approach technically would only apply to functions of infinite length. We, however, approach the application using the general principles of the Slepian series where it can be applied to any function of finite and infinite length.

Xiao attacked the concept by investigating the roots or quadrature nodes of the function set of $\psi_n(c,t)$. In her paper she stated that a function $f(t)$ could be interpolated by the expression

$$f(t) = \rho_1 \psi_1(t) + \rho_2 \psi_2(t) + \cdots + \rho_n \psi_n(t). \tag{56}$$

The coefficients $\{\rho_1, \ldots, \rho_n\}$ were determined by solving an ($n \times n$) linear system of quadrature nodes of $f(t)$. Her results were presented in table form in [24,25]. Equation (56) is analogous to the synthesis of (14), where the equivalent coefficients (analysis) in this paper were calculated using the principles of (2).

Walter uses the principles of (1) and (2) in his approach but his theory only applies under the restriction of where the discrete set $y[k]$ samples of the function is maximally concentrated on the interval $[-t_0, t_0]$. With this, he states that $f(t)$ could be approximately recovered using the following formula:

$$f(t) \simeq \sum_{k=-\tau}^{\tau} y[k] \left\{ \sum_{n=0}^{2\tau} \psi_n[k] \psi_n(t) \right\} \chi_\tau(t). \tag{57}$$

The above is simply a combination of the discrete representation of the analysis (11) and the synthesis (14) for infinite length functions where characteristic function $\chi_\tau(t)$ is added to compensate for the truncation to a finite discrete set of $y[k]$ samples. In his paper [23], he stated that the value τ of (57) is the boundary limit of the finite discrete function $y[k]$ on which it is concentrated and his notation of τ would be the equivalent of c/π or $(t_0\Omega)/\pi$. We have shown experimentally in the empirical results of Section 9 that the truncation value of the series has a dependency on the Slepian frequency c and the cutoff frequency, Ω, of the test function. The bandwidth, c is important because it shares a direct relationship with the cutoff frequency of the discrete set, $y[k]$. The recovery of $f(t)$ using (57) only applies to functions whose energy is mainly concentrated in the interval $[-t_0, t_0]$. To complete the application of PSWFs as an interpolator we must consider the Slepian frequency c and the energy index or the eigenvalue $\lambda_n(c)$ of $\psi_n(c,t)$.

When discussing finite-length discrete data sets, the ideas of Walter [23] are correct when it comes to interpolating these sets over a infinite interval. However, when it comes to interpolating data over finite
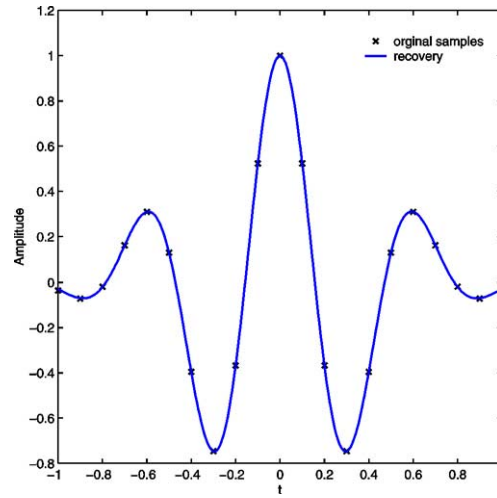
Fig. 8. Results from recovery (solid line) against original (data points) for test function $f(t) = \cos(10t)e^{-\pi t^2}$.

sets we present a more general approach by using the foundations of the Slepian series. By applying the general principles (40), (41) and (42) we can interpolate any discrete bandlimited function over any interval $[-t_0, t_0]$. By implementing (27) in a discrete sense and substituting it into (28), $f(t)$ can be recovered by using the following interpolation formula:

$$f(t) = \frac{t_0}{M} \sum_{k=-M}^{M} y[k] \sum_{n=0}^{\infty} \frac{\psi_{n,c}[k]\psi_n(c,t)}{\lambda_n(c)}. \tag{58}$$

The advantage that this technique has over the method implemented by Xiao [24], [25] is that similarly to the Shannon sampling theorem, (58) can be implemented on equidistant data points. The Xiao technique of Gaussian quadrature nodes is restricted to sampling points equal to the zero crossings of a given PSWF. This limits the number of real life problems her method can be used for. Although, in her paper she empirically shows her approach to be formidable over other Gaussian interpolation schemes.

In Fig. 8, Eq. (58) was tested against a discrete set of $2M = 20$ samples using the test function $f(t) = \cos(10t)e^{-\pi t^2}$. Since the test function was symmetric, only the $\psi_n(c,t)$ of even order n were considered. The Slepian frequency was chosen to be $c = 27$ and the truncation of the series was chosen to be $N' = 10$. As clearly demonstrated, (58) provides a good approximation of a finite length function independent of the amount of energy contained within the interval $[-t_0, t_0]$ with a mean absolute deviation of $5.72e^{-4}$. When the same test was conducted with the Fourier series with the same number of N expansion coefficients, it achieved a mean absolute deviation of $1.79e^{-3}$.

7. Convergence to the Shannon sampling theorem

If symmetry is not taken into consideration for a given function $f(t)$ in the continuous domain, the analysis equation using the Slepian series is

$$\gamma_n(c) = \lambda_n^{-1}(c) \int_{-t_0}^{t_0} f(t)\psi_n(c, t) \, \mathrm{d}t, \tag{59}$$

and the synthesis equation is

$$f(t) = \sum_{n=0}^{\infty} \gamma_n(c)\psi_n(c, t). \tag{60}$$

The discrete case of (59) and (60), for a given set of length $2M$ discrete values of f, where $k \in [-M, M]$, can be expressed as

$$\gamma_n(c) = \frac{t_0}{M\lambda_n(c)} \sum_{k=-M}^{M} y[k]\psi_{n,c}[k], \tag{61}$$

$$f(t) \simeq \sum_{n=0}^{N} \gamma_n(c)\psi_n(c, t). \tag{62}$$

By substituting (61) into (62), we get

$$f(t) \simeq \frac{t_0}{M} \sum_{n=0}^{N} \frac{\psi_n(c, t)}{\lambda_n(c)} \left\{ \sum_{k=-M}^{M} y[k]\psi_{n,c}[k] \right\}. \tag{63}$$

When the terms of (63) are rearranged, we get the interpolation formula of (58).

The expansion of the sinc function using PSWFs, as found in [4], is

$$\mathrm{sinc}\,\Omega(t - x) = \frac{\pi}{\Omega} \sum_{n=0}^{\infty} \psi_n(c, t)\psi_n(c, x). \tag{64}$$

The equation pair of (61) and (62) concern a discrete set of samples contained within a finite interval. Now let us look at the continuous case where $t \in (-\infty, \infty)$. Given the synthesis of (60) over the entire domain of t, we can write

$$f(t) = \sum_{n=0}^{N} \psi_n(c, t) \int_{-\infty}^{\infty} f(x)\psi_n(c, x) \, \mathrm{d}x, \tag{65}$$

By implementing the integral in (65) in the discrete sense, we obtain

$$f(t) = T_s \sum_{n=0}^{N} \psi_n(c, t) \sum_{k=-\infty}^{\infty} y[k]\psi_{n,c}[k], \tag{66}$$

which can be written as

$$f(t) = T_s \sum_{k=-\infty}^{\infty} y[k] \sum_{n=0}^{N} \psi_n(c, t)\psi_{n,c}[k], \tag{67}$$

where $T_s = \pi/\Omega$ is the sampling period and Ω is the cutoff frequency of the discrete function set. Equation (67) can also be regarded as the Shannon sampling theorem for certain c and as $N \to \infty$, but can be approximated to a good precision for certain N.

When (64) is implemented in a discrete manner within the interval $t \in [-t_0, t_0]$, the following is obtained:

$$\frac{\sin w_c \pi (t/T_s - k)}{\pi (t/T_s - k)} = \frac{w_c \pi t_0}{c} \sum_{n=0}^{N} \psi_n(c, t) \psi_{n,c}[k], \tag{68}$$

where w_c is the normalized cutoff frequency of the sinc function. Notice that the eigenvalue or energy index is very small as it goes well beyond the $\lceil (2\pi)/c \rceil$ cutoff point for increasing n in Tables 5 and 6. It was empirically found that to obtain a good approximation of $(\sin w_c \pi (t/T_s - k))/(\pi (t/T_s - k))$ using (68), the truncation value of the series must be set to $N = \lceil c \rceil$. Anything beyond the truncation level of $\lceil c \rceil$ would contribute very little to the expansion of (68). Due to the symmetry of this expansion, only the first 19 of the total 37 sinc samples are displayed in Table 1. To implement (68), the Slepian frequency c must be set to

$$c = \frac{w_c \pi t_0}{T_s}. \tag{69}$$

At the bottom of each column of this table is the total energy, E_p, of the vectors y_1, y_2, and y_3, which were calculated using Parseval's theorem [15]

$$E_p = \sum_{k=-M}^{M} |y_i[k]|^2. \tag{70}$$

It is important to note that the energy of the sinc expansion, y_3, using (68), when $N = \lceil c/2 \rceil$ is noticeably less than the energy of y_2 for which $N = \lceil c \rceil$. When $N = \lceil c \rceil$, the energy is virtually the same as that of the sampled sinc function of y_1 as is shown in the bottom row of Table 1.

Substituting (68) into (67) and setting $w_c = 1$ gives

$$f(t) = \frac{c T_s}{\pi t_0} \sum_{k=-\infty}^{\infty} y[k] \frac{\sin \pi (t/T_s - k)}{\pi (t/T_s - k)}. \tag{71}$$

Therefore, due to the property of (68), (67) approximates very well to the Shannon sampling theorem when $t \in (-\infty, \infty)$ for $c = (\pi t_0)/T_s$ and $N = \lceil c \rceil$. It is important to reemphasize the fact that c is also equal to the time bandwidth product relationship of Ωt_0. The convergence of the interpolation formula of (67) to the Shannon sampling theorem for all k is more currently useful in the analytical sense. This is because (67) requires knowing $\psi_{n,c}[k]$ for large values of k. Currently there is a lack of knowledge of how PSWFs behave outside the $[-t_0, t_0]$ interval. Slepian made an intensive investigation of this [20].

A good approximation of the sinc function of (68) can be obtained when the truncation value $N = \lceil c \rceil$. When N is lowered, the function that dominates is that of a slightly malformed sinc function. We know that much of the theory in mathematical communication is based on the properties of the sinc function [15]. What this shows us is that it is not the sinc function itself that provides this capability, but rather the 'sinc *like structure*' of any kernel function.

8. Square wave analysis

As the empirical results show, the Slepian series approximation converges more quickly for increasing order n over other well-known orthogonal expansion schemes such as: Fourier, Legendre,

Table 1
Samples of: (i) sinc y_1 against samples of expansion (68), (ii) using $N = \lceil c \rceil$ y_2, (iii) using $N = \lceil c/2 \rceil$ y_3, where $w_c = 0.4$, $T_s = 1/18$, $k = 0$, $t_0 = 1$ and $c = (w_c \pi t_0)/T_s = 22.6$

| t/T_s	y_1	y_2	y_3
-18	-0.010394	-0.010803	-0.003662
-17	0.011006	0.011864	-0.017498
-16	0.018921	0.019808	-0.031301
-15	$-1.56\mathrm{E}{-17}$	$2.50\mathrm{E}{-05}$	-0.029140
-14	-0.021624	-0.022199	-0.005321
-13	-0.014392	-0.014741	0.023396
-12	0.015591	0.015808	0.029285
-11	0.027521	0.027906	0.003029
-10	$-1.56\mathrm{E}{-17}$	$6.40\mathrm{E}{-05}$	-0.030176
-9	-0.033637	-0.033888	-0.031907
-8	-0.023387	-0.023585	0.006451
-7	0.026728	0.026795	0.045775
-6	0.050455	0.050641	0.034839
-5	$-1.56\mathrm{E}{-17}$	$6.90\mathrm{E}{-05}$	-0.029232
-4	-0.075683	-0.075766	-0.080515
-3	-0.062366	-0.062471	-0.036993
-2	0.093549	0.093524	0.115710
-1	0.302730	0.302780	0.292790
0	0.400000	0.400070	0.371110
E_p	0.39443	0.39494	0.37111
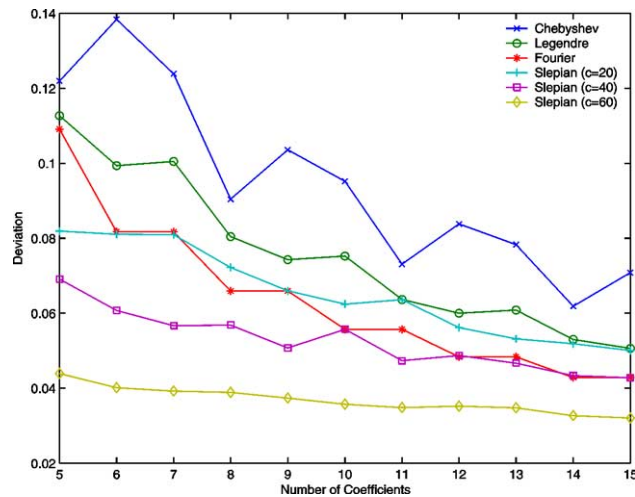
Fig. 9. Mean absolute deviations of square wave using Chebyschev, Legendre, Fourier, Slepian ($c = 20$), Slepian ($c = 40$), Slepian ($c = 60$).

and Chebyschev. This has been particularly shown for discontinuous functions such as the square wave, see Figs. 9 and 10. The advantage the Slepian series approximation has that separates it from many other orthogonal expansions, is the presence of a free continuous tunable parameter, the Slepian frequency c.
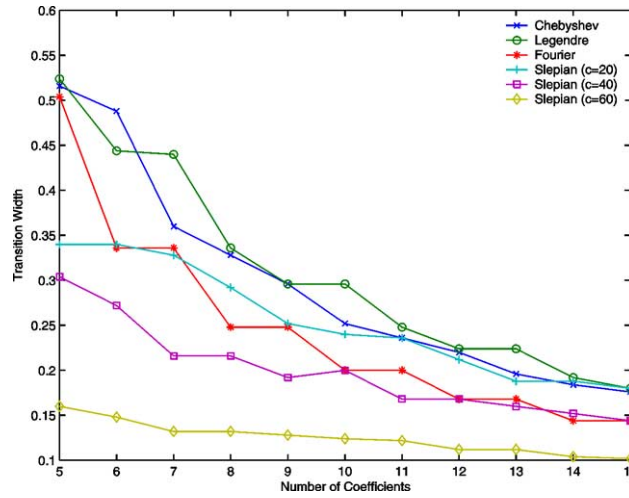
Fig. 10. Transition width of discontinuity of square wave using Chebyschev, Legendre, Fourier, Slepian ($c = 20$), Slepian ($c = 40$), Slepian ($c = 60$).

The empirical results show that the Slepian series approximation converges from orders 5 to 15. The goal of this section is to show analytically that the Slepian series approximation converges to a finite value as the number of terms in the expansion approaches infinity for the square wave function. An analytical expression for $\int_{-t_0}^{t_0} \psi_n(c, t)\, dt$ must first be established. To find this analytical expression we begin with the finite Fourier transform, (7). When Euler's equation is applied to (7), one obtains

$$\int\limits_{-t_0}^{t_0} \psi_n(c,t)\big[\cos(wt) + j\sin(wt)\big]\, dt = (-1)^{\frac{n}{2}}\sqrt{\frac{2\pi\lambda_n(c)t_0}{\Omega}}\,\psi_n\left(c, \frac{wt_0}{\Omega}\right). \tag{72}$$

By setting $w = 0$ in (72) and applying the time-bandwidth product $c = t_0\Omega$

$$\int\limits_{-t_0}^{t_0} \psi_{2n}(c,t)\, dt = t_0(-1)^n\sqrt{\frac{2\pi\lambda_{2n}(c)}{c}}\,\psi_{2n}(c, 0). \tag{73}$$

The analytical expression for (72) for odd orders of n and $w = 0$ is trivial because the integral of an odd function is zero, therefore we need to only consider even order n. Thus an analytical expression for the integrand of $\psi_n(c, t)$ over $t \in [-t_0, t_0]$ is obtained. As an incidental note, an analytical expression for the $v_n(0)$ used in the multitaper F-tests for periodic components is also obtained.

Equation (38) can be rewritten as

$$\sum_{n=0}^{\infty} \lambda_n(c)\big|\gamma_n(c)\big|^2 = \sum_{n=0}^{\infty} \lambda_n(c)\left|\frac{\int_{-t_0}^{t_0} f(t)\psi_n(c,t)\, dt}{\lambda_n(c)}\right|^2. \tag{74}$$

By utilizing (74), the analytical expression of (73) and the following square wave function:

$$f(t) = \begin{cases} 1 & |t| \leqslant 1/2, \\ 0 & \text{otherwise}, \end{cases} \tag{75}$$

the following is obtained:

$$\sum_{n=0}^{\infty} \lambda_n(c) |\gamma_n(c)|^2 = \sum_{n=0}^{\infty} \frac{|((-1)^n/2)\sqrt{(2\pi/c)\lambda_{2n}(c)}\psi_{2n}(c,0)|^2}{\lambda_{2n}(c)}. \tag{76}$$

Therefore, the total energy of the square wave function of (75) is

$$\sum_{n=0}^{\infty} \lambda_n(c) |\gamma_n(c)|^2 = \frac{\pi}{2c} \sum_{n=0}^{\infty} |\psi_{2n}(c,0)|^2. \tag{77}$$

By referring to (13) we can see that the energy of the sequence (77) is convergent for increasing order n, therefore,

$$\lim_{N \to \infty} \frac{\pi}{2c} \sum_{n=0}^{N} |\psi_{2n}(c,0)|^2 = E^c, \tag{78}$$

where E^c is a finite amount of energy. The energy of the square wave approximation converges to a finite value which has a c dependency. What is interesting about (78) is the outcome of $\lim_{c \to \infty} (\pi/2c) \sum_{n=0}^{N} |\psi_{2n}(c,0)|^2$. As our empirical studies and intuition have told us is that $\lim_{c \to \infty} (\pi/2c) \sum_{n=0}^{N} |\psi_{2n}(c,0)|^2$ should be close to zero but never reaching it for fixed N. We have yet to mathematically show this and are currently working on this. This would tell us that N has a dependency on c and changing c will cause more drastic effects on the energy of the analysis coefficients then by increasing the number of terms N in the expansion of the Slepian series approximation of the square wave function.

9. Numerical results

In the experimental results of this paper, all test functions were heavily over sampled to $M = 250$ over the continuous interval of $[-1, 1]$. In Tables 2–4 we compare the Slepian synthesis maneuver of (44) and (46) against: the Fourier series equivalent of (31), the Legendre series equivalent of (33), and the Chebyschev series equivalent of (35). The floating point values within Tables 2–4 represent the mean absolute deviations ε of the various synthesis for even-symmetric functions

$$\varepsilon = \frac{1}{M} \sum_{k=-M}^{M} |y_{\text{act}}[k] - y_{\text{approx}}[k]|, \tag{79}$$

$y_{\text{act}}[k]$ is the actual sample of the original test function where $y_{\text{approx}}[k]$ is the approximation of the sample. In the tables and figures of this section only the even coefficients of the synthesis equations (31), (33), and (35) are counted since all test functions are even.

When performing a Fourier, Legendre, or Chebyschev series synthesis, only the truncation value N' needs to be considered. With the Slepian synthesis, a choice of two parameters is required: the truncation value N' and the Slepian frequency c.

There are several techniques to be considered when it comes to decomposing and reconstructing discrete data sets. One of the most common of these is the Taylor series expansion which is also known

Table 2
Deviations for $e^{-\pi t^2}$ expansion using (i) Chebyschev, (ii) Legendre, (iii) Fourier, and (iv) Slepian ($c = 11$)

c	$n = 3$	$n = 4$	$n = 5$	$n = 6$
(i)	3.0400E–02	5.5524E–03	8.3296E–04	1.0557E–04
(ii)	2.3729E–02	4.4209E–03	6.6906E–04	8.8116E–05
(iii)	3.8071E–03	2.1947E–03	1.5327E–03	1.1260E–03
(iv)	9.1577E–03	1.5079E–03	7.5250E–05	5.1552E–06

Table 3
Deviations for $(t \pm 0.8)(t \pm 0.25)$ expansion using (i) Chebyschev, (ii) Legendre, (iii) Fourier, and (iv) Slepian ($c = 8$)

c	$n = 3$	$n = 4$	$n = 5$	$n = 6$
(i)	3.2374E–17	3.4110E–17	9.6117E–17	1.4733E–16
(ii)	1.9600E–05	3.7966E–05	6.6045E–05	1.0544E–04
(iii)	3.7058E–02	2.2714E–02	1.5350E–02	1.1100E–02
(iv)	8.0226E+01	2.4217E+00	4.9491E–03	3.8473E–02

Table 4
Deviations for triangle expansion using (i) Chebyschev, (ii) Legendre, (iii) Fourier, (iv) Slepian ($c = 15$), (v) Slepian ($c = 30$), and (vi) Slepian ($c = 45$)

c	$n = 5$	$n = 10$	$n = 15$
(i)	2.6296E–02	7.8518E–03	5.5978E–03
(ii)	1.2132E–02	3.6146E–03	1.7735E–03
(iii)	1.1095E–02	2.5683E–03	1.4565E–03
(iv)	7.1719E–03	2.8531E–03	1.5476E–03
(v)	4.9915E–02	1.9872E–03	1.1928E–03
(vi)	9.8471E–02	1.8943E–02	1.1193E–03

Table 5
Table of eigenvalues $\lambda_n(c)$

n	$c = 4$	$c = 6$	$c = 8$	$c = 10$
0	9.958855E–01	9.999019E–01	9.999979E–01	1.000000E+00
1	9.121074E–01	9.960616E–01	9.998790E–01	9.999968E–01
2	5.190548E–01	9.401734E–01	9.970046E–01	9.998927E–01
3	1.102110E–01	6.467919E–01	9.605457E–01	9.979012E–01
4	8.827876E–03	2.073492E–01	7.479028E–01	9.744578E–01
5	3.812917E–04	2.738717E–02	3.202766E–01	8.251463E–01
6	1.095087E–05	1.955001E–03	6.078443E–02	4.401501E–01
7	2.278639E–07	9.484877E–05	6.126289E–03	1.123248E–01
8	3.606549E–09	3.436783E–06	4.182521E–04	1.492017E–02
9	4.493830E–11	9.732116E–08	2.166309E–05	1.314589E–03
10	4.525228E–13	2.218981E–09	8.930427E–07	8.821343E–05
11	3.760303E–15	4.166226E–11	3.013735E–08	4.766445E–06
12	2.622819E–17	6.557479E–13	8.496585E–10	2.133963E–07
13	1.557594E–19	8.780377E–15	2.033408E–11	8.070716E–09
14	7.971108E–22	1.012578E–16	4.185268E–13	2.617019E–10
15	3.551908E–24	1.016384E–18	7.490502E–15	7.363490E–12

Table 6
Table of eigenvalues $\lambda_n(c)$

n	$c = 12$	$c = 14$	$c = 16$	$c = 18$
0	1.000000E+00	1.000000E+00	1.000000E+00	1.000000E+00
1	9.999999E–01	1.000000E+00	1.000000E+00	1.000000E+00
2	9.999967E–01	9.999999E–01	1.000000E+00	1.000000E+00
3	9.999166E–01	9.999971E–01	9.999999E–01	1.000000E+00
4	9.985873E–01	9.999395E–01	9.999978E–01	9.999999E–01
5	9.836643E–01	9.990707E–01	9.999578E–01	9.999983E–01
6	8.817566E–01	9.896394E–01	9.993976E–01	9.999714E–01
7	5.573608E–01	9.217010E–01	9.934676E–01	9.996133E–01
8	1.834293E–01	6.636508E–01	9.490070E–01	9.958984E–01
9	3.105418E–02	2.725476E–01	7.536726E–01	9.672107E–01
10	3.374547E–03	5.777202E–02	3.748451E–01	8.254308E–01
11	2.774189E–04	7.560403E–03	9.834334E–02	4.829847E–01
12	1.847508E–05	7.360924E–04	1.532590E–02	1.552134E–01
13	1.028252E–06	5.809916E–05	1.731059E–03	2.869820E–02
14	4.875879E–08	3.854066E–06	1.577557E–04	3.716451E–03
15	1.998146E–09	2.192371E–07	1.211815E–05	3.841643E–04

to be one of the worst. Orthogonal expansions using the properties of generalized analysis and synthesis have proven to be more reliable, particularly using Chebyschev functions [8]. It is well known that the Fourier synthesis works particularly well with approximating complete trigonometric functions while the Chebyschev and Legendre synthesis works well with approximating polynomials. This can be seen in Table 3 where the Chebyschev approximation of the polynomial $f(t) = (t \pm 0.25)(t \pm 0.8)$ has a formidably faster convergence than any other synthesis tested including the Slepian synthesis.

However, in Table 2, we empirically show that the Slepian series synthesis has a faster convergence on the smooth Gaussian function of $f(t) = e^{-\pi t^2}$. When working with smooth functions of finite length such as $e^{-\pi t^2}$, choosing the optimal Slepian frequency c for the Slepian series is a tricky task. Similarly to the basis sets used in this paper, most orthogonal basis sets do not have a free tuning parameter. In this paper we choose c empirically; there has yet to be developed an analytical method. The only consistency that was found was that the choice of the optimal truncation value N' and the Slepian frequency c at least follow the condition established in (43) where the reasoning had been provided.

Discrete data sets in real world applications (i.e., digital audio) are mostly not that of smooth functions but rather a series of discontinuous values. Perhaps one of the most simplest cases of a discontinuous set is the square wave (75).

Figures 9 and 10 show some statistics of the square wave approximation of (75) using various orthogonal expansions: Fourier, Legendre, Chebyschev, and Slepian ($c = 20$, 40, and 60). In Fig. 9, it is demonstrated that the Slepian synthesis produces significantly smaller mean absolute error for Slepian frequency value $c = 60$ than any other orthogonal approximation. It also shows that as the number of terms in the expansion increases the mean absolute error also decreases. Figure 10 shows the transition width at the discontinuity of (75) for the various approximations. It is also smallest using the Slepian synthesis when $c = 60$, which also decreases for increasing number of coefficients.

10. Conclusion

The intent of this paper was to serve as an introduction to the Slepian series and its properties with some new analytical and empirical results. It was also to serve partially as a review of PSWFs with some new perspectives. Much of the respected literature pertaining to PSWFs focus on the special properties of the energy concentration of these functions in the time and frequency domain. In this paper the focus is shifted more to its orthogonal properties. The authors would also like to stress the single most important advantage that distinguishes the Slepian series from any other orthogonal expansion used in this paper, is the flexibility of a free frequency parameter, the Slepian frequency c. It is interesting to note that no other set orthogonal basis functions posses this bandwidth parameter c which can be tailored to the application. We have shown experimentally that with the use of the Slepian frequency c, the Slepian series synthesis potentially provides more accuracy over the Fourier, Legendre, and Chebyschev synthesis. Intuitively, the Slepian frequency c can be seen as a 'tuning parameter' to provide more control over potential applications, than any other orthogonal basis set.

With regards to interpolation, it is analytically shown that the Slepian analysis/synthesis combination converges to the Shannon sampling theorem under certain settings of the Slepian frequency, c, and truncation level, N. The experimental results illustrated also show that the Slepian series interpolation routine (58) is potentially optimal over the classical Fourier series of the same truncation levels over a finite interval $[-t_0, t_0]$

All results in this paper were generated from a C program written by the first author called SLEPIAN.cpp running from a 400 MHz Celeron microprocessor. Although there are more efficient routines for generating PSWFs, time complexity was not the issue in this paper. More investigation can be applied to any of these ideas presented some of them are currently being pursued in greater detail by the authors of this paper.

Acknowledgments

References

[1] M. Abramowitz, I. Stegen, Handbook of Mathematical Functions with Formulas, Graphs and Mathematical Tables, Addison–Wesley, New York, 1972.

[2] S. Dharanipragada, K.S. Arun, Bandlimited extrapolation using time-bandwidth dimension, IEEE Trans. Signal Process. 45 (1997) 2951–2966.

[3] C. Flammer, Spheroidal Wave Functions, Stanford Univ. Press, Stanford, CA, 1956.

[4] R.B. Frieden, Evaluation, design and extrapolation methods for optical signals, based on use of the prolate functions, Progr. Optics 9 (1971) 313–406.

[5] S. Hanish, R.V. Baier, A.L. VanBuren, B.J. King, Tables of Radial Spheroidal Wave Functions, vol. 1, New York, National Research Laboratory Report 7088, 1970.

[6] A. Katok, B. Hasselblatt, Introduction to the Modern Theory of Dynamical Systems, Cambridge Univ. Press, Cambridge, 1995.

 [7] M. Kozin, V. Volkov, D. Svergun, A compact algorithm for evaluating linear prolate functions, IEEE Trans. Signal Process. 45 (1997) 1075–1077.
 [8] C. Lanczos, Applied Analysis, Prentice Hall, Englewood Cliffs, NJ, 1964.
 [9] H.J. Landau, H.O. Pollack, Prolate spheroidal wave functions, Fourier analysis and uncertainty—II, Bell Syst. Techn. J. 40 (1961) 65–94.
[10] H.J. Landau, H.O. Pollack, Prolate spheroidal wave functions, Fourier analysis and uncertainty—III: the dimension of the space of essentially time and bandlimited signals, Bell Syst. Techn. J. 41 (1962) 1295–1336.
[11] H.J. Landau, H.O. Pollack, The eigenvalue distribution of time and frequency limiting, J. Math. Phys. 77 (1980) 469–481.
[12] L. Li, M. Leong, T. Yeo, P. Kooi, K. Tan, Computations of spheroidal harmonics with complex arguments: a review with an algorithm, Phys. Rev. 58 (1998).
[13] Z. Lin, R.W. McCallum, H. Wang, Computation and Performance of the Prolate-Spheroidal Wave Function Window in Spectral Estimation, 1996.
[14] P.M. Morse, H. Feshbach, Methods of Theoretical Physics, McGraw–Hill, New York, 1953.
[15] A.V. Oppenhiem, R.W. Schafer, Discrete-Time Signal Processing, second ed., Prentice Hall, Englewood Cliffs, NJ, 1999.
[16] D.B. Percival, A.T. Walden, Spectral Analysis for Physical Applications: Multitaper and Conventional Univariate Techniques, Cambridge Univ. Press, Cambridge, 1993.
[17] M.S. Sabri, W. Steenhaart, An approach to band-limited signal extrapolation: the extrapolation matrix, IEEE Trans. Circ. Syst. 25 (1978) 74–78.
[18] D. Slepian, H.O. Pollack, Prolate spheroidal wave functions, Fourier analysis, and uncertainty—I, Bell Syst. Techn. J. 40 (1961) 43–63.
[19] D. Slepian, Prolate spheroidal wave functions, Fourier analysis and uncertainty—IV: extensions to many dimensions; generalized prolate spheroidal functions, Bell Syst. Techn. J. 43 (1962) 3009–3057.
[20] D. Slepian, Some asymptotic expansions for prolate spheroidal wave functions, J. Math. Phys. 44 (1965) 99–140.
[21] J.A. Stratton, P.M. Morse, L.J. Chu, J.D.C. Little, Spheroidal Wave Functions, Technology Press of MIT, Massachusetts, 1957.
[22] T. Verma, S. Bilbao, T. Meng, The digital prolate spheroidal window, in: IEEE International Conference on Acoustics, Speech, and Signal Processing (ICASSP-96), vol. 3, 1996, pp. 1351–1354.
[23] G. Walter, X. Shen, Sampling with prolate spheroidal wave functions, J. Sampling Theor. Signal Image Process. 2 (2003) 25–52.
[24] H. Xiao, V. Roklin, N. Yarvin, Prolate spheroidal wave functions, quadrature and interpolation, Inverse Problems 17 (2001) 805–838.
[25] H. Xiao, Prolate spheroidal wave functions, quadrature, interpolation, and asymptotic formulae, Ph.D. dissertation, Yale University, Department of Computing Science, 2001.
[26] S. Zhang, J.M. Jin, Computation of Special Functions, Wiley, New York, 1996.